REPORT DOCUMENTATION PAGE

Form Approved OMB NO. 0704-0188

1. REPORT DATE (DD-MM-YYYY)	2. REPORT TYPE	3. DATES COVERED (From - To)
27-07-2012	Conference Proceeding	-

4. TITLE AND SUBTITLE
Statistical Efficiency of Simultaneous Target and Sensors Localizationwith Position Dependent Noise

5a. CONTRACT NUMBER
W911NF-10-1-0369

5b. GRANT NUMBER

5c. PROGRAM ELEMENT NUMBER
611102

6. AUTHORS
R. W. Osborne, III, Y. Bar-Shalom, J. George, L. Kaplan

5d. PROJECT NUMBER

5e. TASK NUMBER

5f. WORK UNIT NUMBER

7. PERFORMING ORGANIZATION NAMES AND ADDRESSES
University of Connecticut - Storrs
Office for Sponsored Programs
University of Connecticut
Storrs, CT 06269 -1133

8. PERFORMING ORGANIZATION REPORT NUMBER

9. SPONSORING/MONITORING AGENCY NAME(S) AND ADDRESS(ES)
U.S. Army Research Office
P.O. Box 12211
Research Triangle Park, NC 27709-2211

10. SPONSOR/MONITOR'S ACRONYM(S)
ARO

11. SPONSOR/MONITOR'S REPORT NUMBER(S)
57823-CS.37

12. DISTRIBUTION AVAILIBILITY STATEMENT
Approved for public release; distribution is unlimited.

13. SUPPLEMENTARY NOTES
The views, opinions and/or findings contained in this report are those of the author(s) and should not contrued as an official Department of the Army position, policy or decision, unless so designated by other documentation.

14. ABSTRACT
This work derives the Cramer-Rao lower bound (CRLB) for an acoustic target and sensor localization system in which the noise characteristics depend on the location of the source. The system itself has been previously examined, but without deriving the CRLB and showing the statistical efficiency of the estimator used. Two different versions of the CRLB are derived, one in which direction of arrival (DOA) and range measurements are available ("full-position CRLB"), and one in which only DOA measurements are available ("bearing-only

15. SUBJECT TERMS
Simultaneous Target and Sensors Localizationwith Position Dependent Noise, Statistical Efficiency

16. SECURITY CLASSIFICATION OF:			17. LIMITATION OF ABSTRACT	15. NUMBER OF PAGES	19a. NAME OF RESPONSIBLE PERSON
a. REPORT	b. ABSTRACT	c. THIS PAGE			Yaakov Bar-Shalom
UU	UU	UU	UU		19b. TELEPHONE NUMBER 860-486-4823

Report Title

Statistical Efficiency of Simultaneous Target and Sensors Localizationwith Position Dependent Noise

ABSTRACT

This work derives the Cramer-Rao lower bound (CRLB) for an acoustic target and sensor localization system in which the noise characteristics depend on the location of the source. The system itself has been previously examined, but without deriving the CRLB and showing the statistical efficiency of the estimator used. Two different versions of the CRLB are derived, one in which direction of arrival (DOA) and range measurements are available ("full-position CRLB"), and one in which only DOA measurements are available ("bearing-only CRLB"). In both cases, the estimator is found to be statistically efficient; but, depending on the sensor-target geometry, the range measurements may or may not significantly contribute to the accuracy of target localization.

Conference Name: SPIE Conf.\ on Signal Proc.,Sensor Fusion, and Target Recognition

Conference Date: April 16, 2012

Statistical Efficiency of Simultaneous Target and Sensors Localization with Position Dependent Noise

Richard W. Osborne, III[a], Yaakov Bar-Shalom[a], Jemin George[b] and Lance Kaplan[b]

[a]Electrical and Computer Engineering Department, University of Connecticut

[b]U.S. Army Research Laboratory

ABSTRACT

This work derives the Cramer-Rao lower bound (CRLB) for an acoustic target and sensor localization system in which the noise characteristics depend on the location of the source. The system itself has been previously examined, but without deriving the CRLB and showing the statistical efficiency of the estimator used. Two different versions of the CRLB are derived, one in which direction of arrival (DOA) and range measurements are available ("full-position CRLB"), and one in which only DOA measurements are available ("bearing-only CRLB"). In both cases, the estimator is found to be statistically efficient; but, depending on the sensor-target geometry, the range measurements may or may not significantly contribute to the accuracy of target localization.

Keywords: CRLB, FIM, estimator efficiency, acoustic localization, fusion

1. INTRODUCTION

In any estimation system the ultimate goal is to extract the maximum information from the available data. The Fisher information matrix (FIM) provides a measure of the total information available from the observations of the system, and its inverse provides the Cramer-Rao lower bound (CRLB) [1]. A statistically efficient estimator is one in which the variance of the estimation error meets the CRLB, and, therefore, extracts all of the available information from the observations.

The CRLB and statistical efficiency of an acoustic localization system will be examined here, based on the system described in [6], which is meant to estimate the location of the source of a detected gunshot. Each sensor node of the system is assumed to provide an estimated bearing (DOA) to the target, and, if the sensor node lies within a certain field-of-view (FOV), a range estimate and bullet trajectory estimate as well. For those sensors which provide estimated range, the noise term will be dependent on the position of the source. Each sensor node's estimates are passed to a fusion center to perform the overall estimation of the target position by fusing all the local estimates.

A number of papers have examined the problem of target localization in passive sensor environments, including [2, 4, 5, 8, 10–12]. The work of [11] generalizes the results of [4] to include sensor position uncertainty, however, neither paper examines the CRLB to see whether the estimator is statistically efficient. In [2, 5, 8, 12], different applications of localization with passive sensors are studied which also consider the CRLB. However, in [12], no estimation scheme is shown to meet the CRLB. In [5] the ML estimation scheme examined is shown to be statistically efficient only when a significant number of measurements are utilized. In none of the previously mentioned papers were cases of position dependent measurement noise considered.

In this work, the CRLB of the central estimator (fuser) is derived for two cases: a "bearing-only" case, which assumes that no range estimates are available from the sensor nodes, and a "full-position" case, which assumes that range estimates *are* available in addition to the DOA.

Section 2 provides an overview of the system in question. Section 3 provides the expressions necessary to evaluate the CRLB for the problem in question, both with and without the position dependent noise terms. Section 4 describes the simulation scenarios and provides the results. Finally, Section 5 concludes the paper.

Proc. SPIE Conf. on Signal Proc., Sensor Fusion and Target Recognition, #8392-2, Baltimore, MD, April 2012.
Sponsored by grants ARO W911NF-10-1-0369, ONR N00014-10-1-0029.

email: [a]{rosborne, ybs}@engr.uconn.edu, [b]{jemin.george, lance.m.kaplan}@us.army.mil

2. LOCALIZATION SYSTEM OVERVIEW

The system to be examined here will be identical to the one described in [6]. A brief overview of the system will be provided here to introduce the concepts and notations.

A number of acoustic sensors are placed throughout a surveillance region with the intent of detecting gunfire and estimating the position of the source. The target (source) location will be denoted as

$$T = \begin{bmatrix} T_x \\ T_y \end{bmatrix} \tag{1}$$

and the ith sensor location will be denoted as

$$S_i = \begin{bmatrix} S_{i_x} \\ S_{i_y} \end{bmatrix} \tag{2}$$

The problem will be assumed constrained to a two-dimensional plane for simplicity.

2.1 Sensor Nodes

Each sensor will provide at most five measurements (local estimates): the DOA angle to the shooter $\hat{\phi}_i$, based on the detection of the muzzle blast, the DOA angle of the shockwave from the bullet $\hat{\varphi}_i$, the time difference of arrival (TDOA) between the muzzle blast and the shockwave $\hat{\tau}_i$, and the sensor location $\hat{S}_{i_x}$ and $\hat{S}_{i_y}$ (through a GPS sensor at each node). Each measurement is assumed to be corrupted by zero-mean Gaussian noise, with standard deviations of σ_ϕ, σ_φ, σ_τ, σ_{i_x} and σ_{i_y}, respectively. The shockwave (and therefore the TDOA measurement) will only be visible to sensor nodes which are within a limited field-of-view (FOV) around the path of the bullet. The FOV will be $\pi - 2\theta$, where

$$\theta = \sin^{-1}\left(\frac{1}{m}\right) \tag{3}$$

and m is the Mach number of the bullet, assumed here to be $m = 2$ [7].

The target bearing from the ith sensor node is

$$\phi_i = \tan^{-1}\left(\frac{T_y - S_{i_y}}{T_x - S_{i_x}}\right) \tag{4}$$

and the DOA angle of the shockwave is

$$\varphi_i = \begin{cases} -\frac{\pi}{2} - \theta + \omega & \text{if } \pi + \omega < \phi_i < \frac{3\pi}{2} - \theta + \omega \\ \frac{\pi}{2} + \theta + \omega & \text{if } \frac{\pi}{2} + \theta + \omega < \phi_i < \pi + \omega \end{cases} \tag{5}$$

where ω is the angle of the trajectory (counter-clockwise) with respect to the x-axis.

Sensor i will pass on the local estimates[1]

$$z_i = \begin{bmatrix} \hat{\phi}_i \\ \hat{r}_i \\ \hat{\omega}_i \end{bmatrix} \quad \text{and} \quad \hat{S}_i = \begin{bmatrix} \hat{S}_{i_x} \\ \hat{S}_{i_y} \end{bmatrix} \tag{6}$$

to a fusion center, where $\hat{\phi}_i$ is the estimated target bearing, $\hat{r}_i$ is the estimated target range obtained from $\hat{\varphi}_i$ and $\hat{\tau}_i$ using (7), and $\hat{\omega}_i$ is the estimated bullet trajectory angle. In view of (5), the estimated bullet trajectory can be obtained directly from $\hat{\varphi}_i$ and the standard deviation of $\hat{\omega}_i$ will be σ_φ.

The estimated range will be [6]

$$\hat{r}_i = \frac{c\hat{\tau}_i}{1 - \cos\left(\hat{\phi}_i - \hat{\varphi}_i\right)} \tag{7}$$

[1] We use similar notation and terminology as in [6].

where c is the speed of sound (assumed to be known perfectly). The variance of the range estimate — which is dependent on both range and bearing — can be approximated as [6]

$$\sigma^2_{r_i}(T, S_i, \omega) \approx \frac{c^2\sigma^2_\tau + r_i^2(\sigma^2_\phi + \sigma^2_\varphi)\sin^2(\phi_i - \varphi_i)}{\big(1 - \cos(\phi_i - \varphi_i)\big)^2} \tag{8}$$

The likelihood functions corresponding to the estimates z_i and $\hat{S}_i$ are

$$p\big(z_i|T, S_i, \omega\big) = \mathcal{N}(z_i; \mu_{z_i}, \Sigma_{z_i}) \tag{9}$$

where

$$\mu_{z_i} = \begin{bmatrix}\phi_i \\ r_i \\ \omega\end{bmatrix} \quad \text{and} \quad \Sigma_{z_i} = \begin{bmatrix}\sigma^2_\phi & 0 & 0 \\ 0 & \sigma^2_{r_i}(T, S_i, \omega) & 0 \\ 0 & 0 & \sigma^2_\varphi\end{bmatrix} \tag{10}$$

and

$$p\big(\hat{S}_i|S_i\big) = \mathcal{N}(\hat{S}_i; S_i, \Sigma_{S_i}) \tag{11}$$

where

$$\Sigma_{S_i} = \begin{bmatrix}\sigma^2_{i_x} & 0 \\ 0 & \sigma^2_{i_y}\end{bmatrix} \tag{12}$$

The errors in (9) and (11) are assumed to be uncorrelated at each sensor and across the sensors.

The sensors are assumed to obtain their locations, albeit imperfectly, from GPS. [2] If desired, the algorithm can perform simultaneous localization of the target and sensors. For the sensors, the GPS localization serves as a prior and guarantees complete observability for the target-sensor complex. The final estimates of the sensor locations can be slightly improved over their initial GPS estimates, but the improvement this makes to the final target localization is negligible.

2.2 Centralized Fusion

The estimates z_i and $\hat{S}_i$ from each sensor are passed on to a fusion center in order to determine the estimate $\hat{\mathbf{x}}$ by means of the Iterated Least Squares (ILS) estimator [1]. The parameter vector to be estimated is

$$\mathbf{x} = \begin{bmatrix}T_x & T_y & \omega & S_{1_x} & S_{1_y} & \dots & S_{n_x} & S_{n_y}\end{bmatrix}' \tag{13}$$

with observations

$$\hat{\mathbf{y}} = \begin{bmatrix}\hat{\mathbf{y}}_1 \\ \vdots \\ \hat{\mathbf{y}}_n\end{bmatrix} \tag{14}$$

where

$$\hat{\mathbf{y}}_i = \begin{bmatrix}z_i \\ \hat{S}_i\end{bmatrix} \tag{15}$$

In order to utilize the ILS estimation algorithm, an initial estimate of $\mathbf{x}$ is needed. It has been noted [6] that the ILS estimator is sensitive to the initial estimate and may diverge if the initial estimate is too far from the truth.

While the initialization of the target position could be performed by using the bearing and range measurements (using the nodes with range measurements), the large variance of the range measurements was found to occasionally cause divergence in the ILS algorithm. A more robust initialization was found to follow a similar

[2] If the sensor position estimates contain a common bias across sensors, the relative sensor registration will be unaffected and the target estimate will exhibit the same bias.

method to that used in [3]. This method of initialization will utilize only the available bearing measurements from each sensor (4), which can be rewritten as

$$\underbrace{\begin{bmatrix} \tan\phi_1 & -1 \\ \tan\phi_2 & -1 \\ \vdots & \vdots \\ \tan\phi_n & -1 \end{bmatrix}}_{A} T = \underbrace{\begin{bmatrix} S_{1_x}\tan\phi_1 - S_{1_y} \\ S_{2_x}\tan\phi_2 - S_{2_y} \\ \vdots \\ S_{n_x}\tan\phi_n - S_{n_y} \end{bmatrix}}_{b} \tag{16}$$

and T can be solved as

$$T = A^{\dagger} b \tag{17}$$

where $A^{\dagger}$ is the (right) pseudo-inverse of A.

Also, note that (16) can be rewritten utilizing the expression

$$\phi_i = \cot^{-1}\left(\frac{T_x - S_{i_x}}{T_y - S_{i_y}}\right) \tag{18}$$

which is simply (4) rewritten using the cotangent function. As suggested in [3], use of the cotangent function has been made when the measured bearing is between 45° and 135° or between -45° and -135°.

To complete the initialization of $\mathbf{x}$, S_i can be taken as $\hat{S}_i$ and ω can be taken as the average of $\hat{\omega}_i$.

3. CRAMER-RAO LOWER BOUND

The CRLB provides a lower bound on the covariance matrix of the estimate $\hat{\mathbf{x}}$ as

$$E\left[(\hat{\mathbf{x}} - \mathbf{x})(\hat{\mathbf{x}} - \mathbf{x})'\right] \geq J^{-1} \tag{19}$$

where J is the Fisher information matrix (FIM)

$$J = E\left\{[\nabla_{\mathbf{x}}\lambda(\mathbf{x})][\nabla_{\mathbf{x}}\lambda(\mathbf{x})]'\right\} \tag{20}$$

and $\lambda(\mathbf{x})$ is the negative log-likelihood function (NLLF)

$$\lambda(\mathbf{x}) = \sum_{i=1}^{n}\left[\frac{1}{2}(z_i - \mu_{z_i}(\mathbf{x}))'\,\Sigma_{z_i}(\mathbf{x})^{-1}(z_i - \mu_{z_i}(\mathbf{x})) + \frac{1}{2}\left(\hat{S}_i - S_i\right)'\Sigma_{S_i}^{-1}\left(\hat{S}_i - S_i\right) + \ln\big(\sigma_{r_i}(\mathbf{x})\big)\right] \tag{21}$$

with the unnecessary constant terms omitted.

In view of (6), (10), and (12), the NLLF can be written as[3]

$$\lambda(\mathbf{x}) = \frac{1}{2}\sum_{i=1}^{n}\Bigg[\frac{1}{\sigma_\phi^2}\left(\hat{\phi}_i - \phi_i\right)^2 + \frac{1}{\sigma_{r_i}^2(T,S_i,\omega)}(\hat{r}_i - r_i)^2 + \frac{1}{\sigma_\varphi^2}(\hat{\omega}_i - \omega)^2 + \frac{1}{\sigma_{i_x}^2}\left(\hat{S}_{i_x} - S_{i_x}\right)^2 + \frac{1}{\sigma_{i_y}^2}\left(\hat{S}_{i_y} - S_{i_y}\right)^2 + \ln\left(\sigma_{r_i}^2(T,S_i,\omega)\right)\Bigg] \tag{22}$$

Note that the noise term for the ith sensor node's range estimate is dependent on the target-sensor geometry.

In order to deal with the position dependent noise term, the "full-position" FIM corresponding to (22) will be broken into "bearing-only"[4] and "range-only" FIMs

$$J = J_b + J_r \tag{23}$$

where J_b denotes the "bearing-only" FIM calculated when ignoring the range term of (22); and J_r denotes the "range-only" FIM calculated for only the range portion of (22).

Two versions of the CRLB will be evaluated in the sequel: the bearing-only CRLB, J_b^{-1}, and the full-position CRLB, J^{-1}.

[3]Note that ω is decoupled from the remaining terms of $\mathbf{x}$, and the ML estimation of ω amounts to simple averaging, with a CRLB of σ_φ^2/n.

[4]This is a slight misnomer since the sensor position terms will also be included in the bearing-only FIM.

3.1 Bearing-Only FIM

The bearing-only FIM J_b will be straightforward, as none of the variances in this case are dependent on $\mathbf{x}$. The gradient of (22), necessary for calculation of the FIM, is detailed in Appendix B. The necessary terms to calculate the FIM are

$$E\left\{\frac{\partial\lambda}{\partial T_x}\frac{\partial\lambda}{\partial T_x}\right\} = \sum_{i=1}^{n}\frac{1}{\sigma_\phi^2}\left(\frac{T_y - S_{i_y}}{r_i^2}\right)^2 \tag{24}$$

$$E\left\{\frac{\partial\lambda}{\partial T_x}\frac{\partial\lambda}{\partial T_y}\right\} = -\sum_{i=1}^{n}\frac{1}{\sigma_\phi^2}\left(\frac{T_y - S_{i_y}}{r_i^2}\right)\left(\frac{T_x - S_{i_x}}{r_i^2}\right) \tag{25}$$

$$E\left\{\frac{\partial\lambda}{\partial T_x}\frac{\partial\lambda}{\partial \omega}\right\} = 0 \tag{26}$$

$$E\left\{\frac{\partial\lambda}{\partial T_x}\frac{\partial\lambda}{\partial S_{i_x}}\right\} = -\frac{1}{\sigma_\phi^2}\left(\frac{T_y - S_{i_y}}{r_i^2}\right)^2 \tag{27}$$

$$E\left\{\frac{\partial\lambda}{\partial T_x}\frac{\partial\lambda}{\partial S_{i_y}}\right\} = \frac{1}{\sigma_\phi^2}\left(\frac{T_y - S_{i_y}}{r_i^2}\right)\left(\frac{T_x - S_{i_x}}{r_i^2}\right) \tag{28}$$

$$E\left\{\frac{\partial\lambda}{\partial T_y}\frac{\partial\lambda}{\partial T_y}\right\} = \sum_{i=1}^{n}\frac{1}{\sigma_\phi^2}\left(\frac{T_x - S_{i_x}}{r_i^2}\right)^2 \tag{29}$$

$$E\left\{\frac{\partial\lambda}{\partial T_y}\frac{\partial\lambda}{\partial \omega}\right\} = 0 \tag{30}$$

$$E\left\{\frac{\partial\lambda}{\partial T_y}\frac{\partial\lambda}{\partial S_{i_x}}\right\} = \frac{1}{\sigma_\phi^2}\left(\frac{T_y - S_{i_y}}{r_i^2}\right)\left(\frac{T_x - S_{i_x}}{r_i^2}\right) \tag{31}$$

$$E\left\{\frac{\partial\lambda}{\partial T_y}\frac{\partial\lambda}{\partial S_{i_y}}\right\} = -\frac{1}{\sigma_\phi^2}\left(\frac{T_x - S_{i_x}}{r_i^2}\right)^2 \tag{32}$$

$$E\left\{\frac{\partial\lambda}{\partial \omega}\frac{\partial\lambda}{\partial \omega}\right\} = \frac{n}{\sigma_\varphi^2} \tag{33}$$

$$E\left\{\frac{\partial\lambda}{\partial \omega}\frac{\partial\lambda}{\partial S_{i_x}}\right\} = 0 \tag{34}$$

$$E\left\{\frac{\partial\lambda}{\partial \omega}\frac{\partial\lambda}{\partial S_{i_y}}\right\} = 0 \tag{35}$$

$$E\left\{\frac{\partial\lambda}{\partial S_{i_x}}\frac{\partial\lambda}{\partial S_{i_x}}\right\} = \frac{1}{\sigma_\phi^2}\left(\frac{T_y - S_{i_y}}{r_i^2}\right)^2 + \frac{1}{\sigma_{i_x}^2} \tag{36}$$

$$E\left\{\frac{\partial\lambda}{\partial S_{i_x}}\frac{\partial\lambda}{\partial S_{i_y}}\right\} = -\frac{1}{\sigma_\phi^2}\left(\frac{T_y - S_{i_y}}{r_i^2}\right)\left(\frac{T_x - S_{i_x}}{r_i^2}\right) \tag{37}$$

$$E\left\{\frac{\partial\lambda}{\partial S_{i_y}}\frac{\partial\lambda}{\partial S_{i_y}}\right\} = \frac{1}{\sigma_\phi^2}\left(\frac{T_x - S_{i_x}}{r_i^2}\right)^2 + \frac{1}{\sigma_{i_y}^2} \tag{38}$$

The matrix J_b can then be constructed with the appropriate entries from (24)–(38).

3.2 Range-Only FIM

Since the variance of the range estimate from each sensor node (for which the shooter is in the FOV necessary to obtain a range estimate) is dependent on $\mathbf{x}$, the expressions for the entries of the FIM in the range-only case are more complicated. The terms for the gradient of (22) (including the range terms) are detailed in Appendix

C. The necessary terms to calculate the FIM J_r are

$$E\left\{\frac{\partial\lambda}{\partial T_x}\frac{\partial\lambda}{\partial T_x}\right\} = 2\sum_{i=1}^{n} a_i^2 + \sum_{i=1}^{n}\frac{(T_x - S_{i_x})^2}{r_i^2\sigma_{r_i}^2} \tag{39}$$

$$E\left\{\frac{\partial\lambda}{\partial T_x}\frac{\partial\lambda}{\partial T_y}\right\} = 2\sum_{i=1}^{n} a_i b_i + \sum_{i=1}^{n}\frac{(T_x - S_{i_x})(T_y - S_{i_y})}{r_i^2\sigma_{r_i}^2} \tag{40}$$

$$E\left\{\frac{\partial\lambda}{\partial T_x}\frac{\partial\lambda}{\partial \omega}\right\} = 2\sum_{i=1}^{n} a_i c_i \tag{41}$$

$$E\left\{\frac{\partial\lambda}{\partial T_x}\frac{\partial\lambda}{\partial S_{i_x}}\right\} = -2a_i^2 - \frac{(T_x - S_{i_x})^2}{r_i^2\sigma_{r_i}^2} \tag{42}$$

$$E\left\{\frac{\partial\lambda}{\partial T_x}\frac{\partial\lambda}{\partial S_{i_y}}\right\} = -2a_i b_i - \frac{(T_x - S_{i_x})(T_y - S_{i_y})}{r_i^2\sigma_{r_i}^2} \tag{43}$$

$$E\left\{\frac{\partial\lambda}{\partial T_y}\frac{\partial\lambda}{\partial T_y}\right\} = 2\sum_{i=1}^{n} b_i^2 + \sum_{i=1}^{n}\frac{(T_y - S_{i_y})^2}{r_i^2\sigma_{r_i}^2} \tag{44}$$

$$E\left\{\frac{\partial\lambda}{\partial T_y}\frac{\partial\lambda}{\partial \omega}\right\} = 2\sum_{i=1}^{n} b_i c_i \tag{45}$$

$$E\left\{\frac{\partial\lambda}{\partial T_y}\frac{\partial\lambda}{\partial S_{i_x}}\right\} = -2a_i b_i - \frac{(T_x - S_{i_x})(T_y - S_{i_y})}{r_i^2\sigma_{r_i}^2} \tag{46}$$

$$E\left\{\frac{\partial\lambda}{\partial T_y}\frac{\partial\lambda}{\partial S_{i_y}}\right\} = -2b_i^2 - \frac{(T_y - S_{i_y})^2}{r_i^2\sigma_{r_i}^2} \tag{47}$$

$$E\left\{\frac{\partial\lambda}{\partial \omega}\frac{\partial\lambda}{\partial \omega}\right\} = 2\sum_{i=1}^{n} c_i^2 \tag{48}$$

$$E\left\{\frac{\partial\lambda}{\partial \omega}\frac{\partial\lambda}{\partial S_{i_x}}\right\} = -2a_i c_i \tag{49}$$

$$E\left\{\frac{\partial\lambda}{\partial \omega}\frac{\partial\lambda}{\partial S_{i_y}}\right\} = -2b_i c_i \tag{50}$$

$$E\left\{\frac{\partial\lambda}{\partial S_{i_x}}\frac{\partial\lambda}{\partial S_{i_x}}\right\} = 2a_i^2 + \frac{(T_x - S_{i_x})^2}{r_i^2\sigma_{r_i}^2} \tag{51}$$

$$E\left\{\frac{\partial\lambda}{\partial S_{i_x}}\frac{\partial\lambda}{\partial S_{i_y}}\right\} = 2a_i b_i + \frac{(T_x - S_{i_x})(T_y - S_{i_y})}{r_i^2\sigma_{r_i}^2} \tag{52}$$

$$E\left\{\frac{\partial\lambda}{\partial S_{i_y}}\frac{\partial\lambda}{\partial S_{i_y}}\right\} = 2b_i^2 + \frac{(T_y - S_{i_y})^2}{r_i^2\sigma_{r_i}^2} \tag{53}$$

$$E\left\{\frac{\partial\lambda}{\partial S_{i_x}}\frac{\partial\lambda}{\partial S_{j_x}}\right\}\Bigg|_{i\neq j} = 0 \tag{54}$$

$$E\left\{\frac{\partial\lambda}{\partial S_{i_x}}\frac{\partial\lambda}{\partial S_{j_y}}\right\}\Bigg|_{i\neq j} = 0 \tag{55}$$

$$E\left\{\frac{\partial\lambda}{\partial S_{i_y}}\frac{\partial\lambda}{\partial S_{j_y}}\right\}\Bigg|_{i\neq j} = 0 \tag{56}$$

where

$$a_i = \frac{\sin(\phi_i - \varphi_i)}{1 - \cos(\phi_i - \varphi_i)} \left(\frac{\text{sign}(T_x - S_{i_x})(\sigma_\phi^2 + \sigma_\varphi^2) r_i \sin(\varphi_i)}{(1 - \cos(\phi_i - \varphi_i))\sigma_{r_i}^2} - \frac{T_y - S_{i_y}}{r_i^2} \right) \tag{57}$$

$$b_i = -\frac{\sin(\phi_i - \varphi_i)}{1 - \cos(\phi_i - \varphi_i)} \left(\frac{\text{sign}(T_x - S_{i_x})(\sigma_\phi^2 + \sigma_\varphi^2) r_i \cos(\varphi_i)}{(1 - \cos(\phi_i - \varphi_i))\sigma_{r_i}^2} - \frac{T_x - S_{i_x}}{r_i^2} \right) \tag{58}$$

$$c_i = \frac{r_i^2(\sigma_\phi^2 + \sigma_\varphi^2) \sin(\phi_i - \varphi_i) \cos(\phi_i - \varphi_i)}{(1 - \cos(\phi_i - \varphi_i))^2 \sigma_{r_i}^2} - \frac{\sin(\phi_i - \varphi_i)}{1 - \cos(\phi_i - \varphi_i)} \tag{59}$$

The matrix J_r can then be constructed with the appropriate entries from (39)–(56).

4. SIMULATION RESULTS

The simulation scenarios examined here include the scenarios of [6] and an additional modified scenario with fewer sensors. For each scenario, the Mach number of the bullet is assumed to be $m = 2$, and the speed of sound is assumed to be $c = 342\,\text{m/sec}$. The measurement noise standard deviations are $\sigma_\phi = \sigma_\varphi = 4^\circ$, $\sigma_\tau = 1\,\text{ms}$, and $\sigma_{i_x} = \sigma_{i_y} = 2\,\text{m}$. The simulations were performed for 100 Monte Carlo runs for each scenario.

In Scenarios 1 and 2, there are five sensor nodes located at

$$S = \begin{bmatrix} 127 & 20 & 90 & 136 & 182 \\ 107 & 22 & 0 & 68 & 59 \end{bmatrix} \tag{60}$$

In Scenario 1, the target is located at $T = \begin{bmatrix} 50 & 50 \end{bmatrix}'$ and the bullet is fired at a trajectory of $\omega = 30^\circ$ (counter-clockwise from the x-axis). Due to the location of the sensors and the trajectory of the bullet, only sensors 1, 4 and 5 receive the shockwave and are able to send range and bullet trajectory estimates to the fusion center.

The results of Scenario 1 are shown in Figure 1 and 2. Each figure shows the true locations of the target and sensors, along with the corresponding 95% error ellipses. Figure 1 shows the error ellipses corresponding to the sample covariance matrix calculated from the estimation errors over the 100 Monte Carlo runs when range measurements are not available at the fusion center (dashed line), and the covariance matrix from the bearing-only CRLB (solid line). Figure 2 shows the covariance matrix calculated from the estimation errors when both range and bearing data are available at the fusion center, and the covariance matrix from the full-position CRLB.

The covariance matrices from the bearing-only CRLB and the full-position CRLB closely match the covariances of the estimation errors calculated from the simulation. This first indicates that the ILS estimation carried out by the fusion center is statistically efficient. Additionally, the fact that the two CRLB matrices closely match suggests that very little information is gained from the range estimates sent from sensors 1, 4 and 5. This is due to the fact that the target-sensor geometry is such that the target bearing measurements alone can achieve good localization.

In Scenario 2, the target is located at $T = \begin{bmatrix} 150 & -50 \end{bmatrix}'$ and the bullet is fired at a trajectory of $\omega = 170^\circ$. Due to the location of the sensors and the trajectory of the bullet, only sensors 2 and 3 receive the shockwave and are able to send range and bullet trajectory estimates to the fusion center.

The results of Scenario 2 are shown in Figures 3 and 4. Each figure once again shows the various 95% error ellipses. Figure 3 shows the error ellipses of the bearing-only CRLB and the estimation errors when range measurements are not available at the fusion center. Figure 4 shows the error ellipses of the full-position CRLB and the estimation errors when both range and bearing data are available at the fusion center.

The covariance matrices from both cases of the CRLB again closely match those obtained from the estimation errors, indicating that the estimator is once again efficient and the range estimates carry very little information.

Scenario 3 consists of an identical situation to Scenario 1, but with sensors 2 and 3 removed. In this case, the geometry of the sensors and target are poor, with each sensor having very similar line-of-sight (LOS) angles to the target.

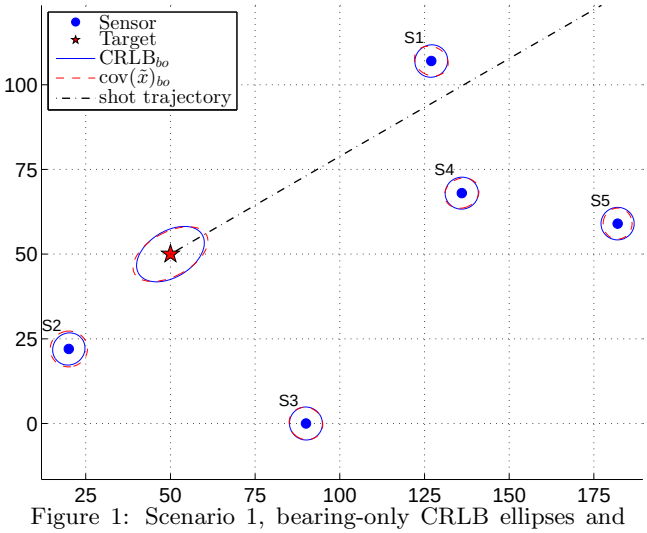

Figure 1: Scenario 1, bearing-only CRLB ellipses and error ellipses of estimated target and sensor locations (all 95%).

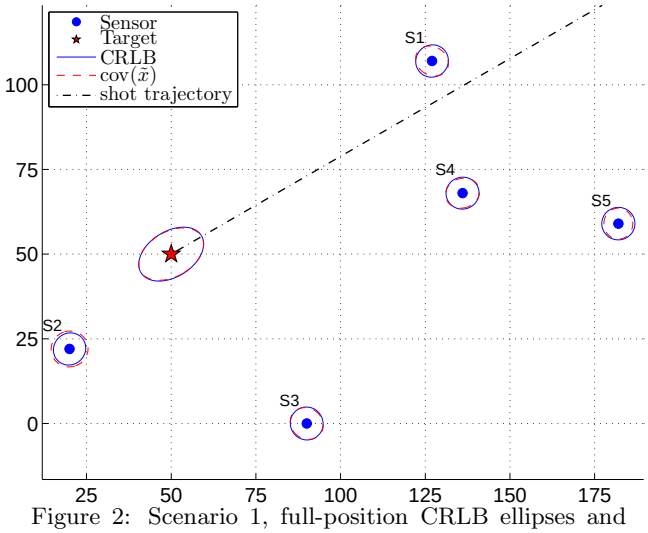

Figure 2: Scenario 1, full-position CRLB ellipses and error ellipses of estimated target and sensor locations (all 95%)

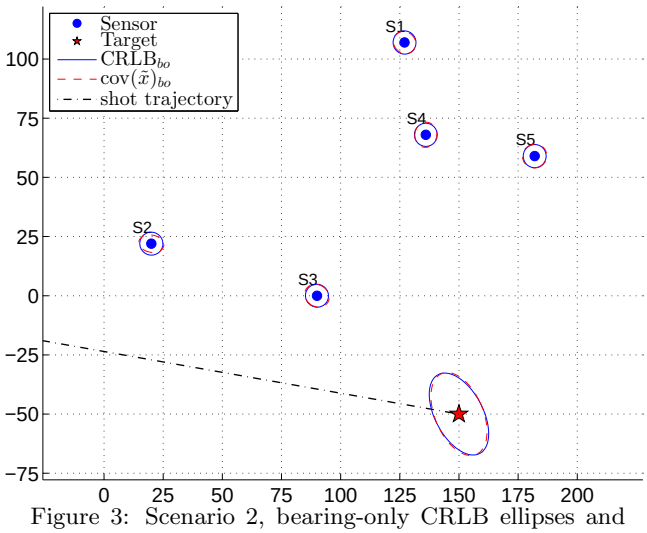

Figure 3: Scenario 2, bearing-only CRLB ellipses and error ellipses of estimated target and sensor locations (all 95%).

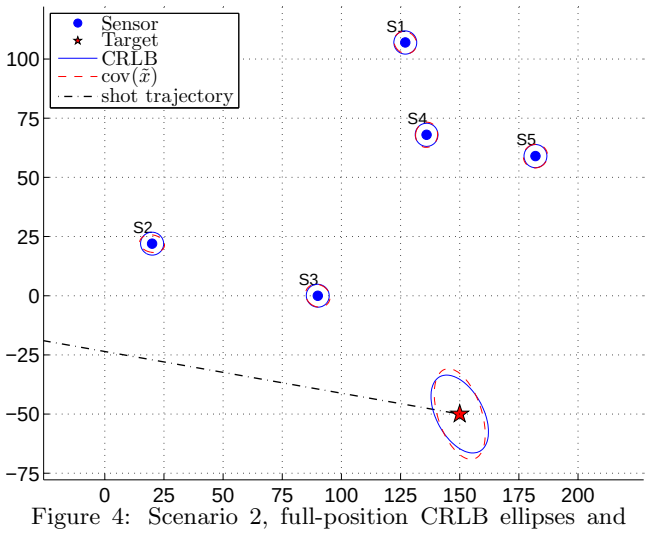

Figure 4: Scenario 2, full-position CRLB ellipses and error ellipses of estimated target and sensor locations (all 95%).

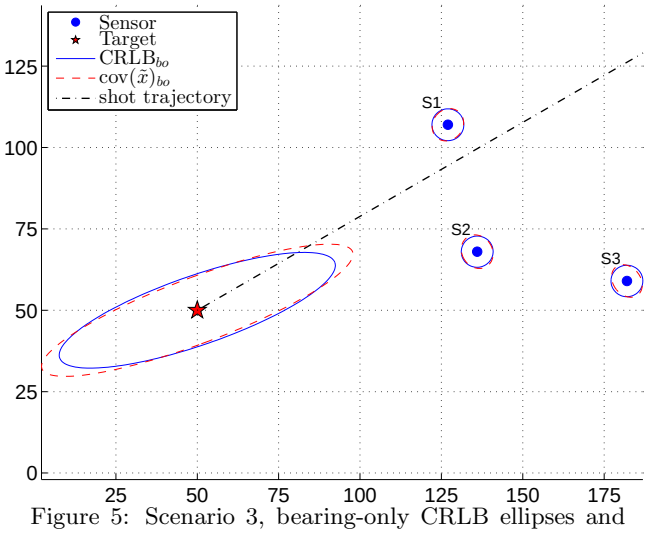

Figure 5: Scenario 3, bearing-only CRLB ellipses and error ellipses of estimated target and sensor locations (all 95%).

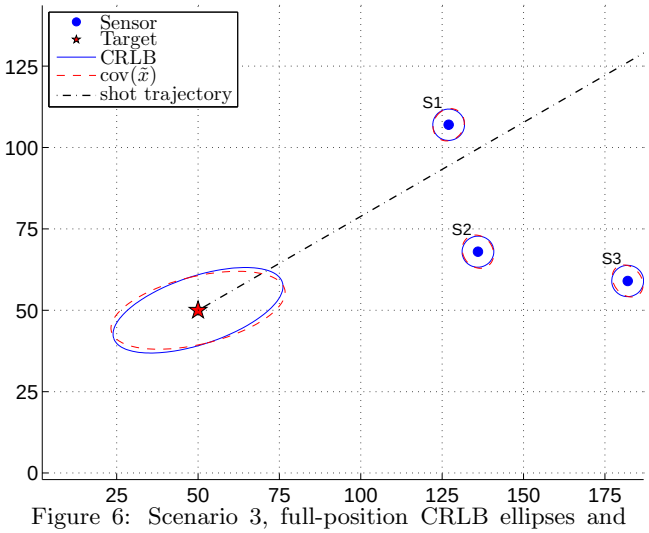

Figure 6: Scenario 3, full-position CRLB ellipses and error ellipses of estimated target and sensor locations (all 95%).

Table 1: Normalized Estimation Error Squared (NEES) (95% probability region is [1.63, 2.41]).

	NEES($\hat{T}_{bo}$)	NEES($\hat{T}$)	NEES($\hat{T}$) wrt CRLB$_{bo}$
Scenario 1	1.95	2.10	1.84
Scenario 2	2.16	1.97	2.00
Scenario 3	2.12	2.20	1.41

The results of Scenario 3 are shown in Figures 5 and 6. In this case, the error ellipses for the bearing-only CRLB and the full-position CRLB no longer coincide. The covariance of the estimation errors closely match their respective CRLB matrices, again indicating that the estimator is efficient.

Additionally, the normalized estimation error squared (NEES) for the source localization was examined for each scenario, using both the bearing-only CRLB and the full-position CRLB to provide a statistical confirmation of the efficiency of the estimator. In each case, the CRLB was evaluated at the true $\mathbf{x}$. The NEES was calculated for

(i) the fused position estimation errors using bearing-only measurements with the bearing-only CRLB,

(ii) the fused position estimation errors using full-position measurements with the full-position CRLB, and

(iii) the fused position estimation errors using full-position measurements with the bearing-only CRLB (to quantify the benefit of range measurements).

The NEES results (with the 95% probability region based on the chi-square distribution with two degrees of freedom and 100 Monte Carlo runs [1], being [1.63, 2.41]) are in Table 1. The first two columns (case (i) and (ii) above) show that in all scenarios, with bearing-only or full position, the fused estimate of the target (source) position matches the CRLB, i.e., it is statistically efficient.

The third column (case (iii) above) shows that the target position errors with full position measurements match in Scenario 1 and 2 the bearing-only CRLB, i.e., the range availability does not contribute to the accuracy of the fused estimate. However, in Scenario 3, the availability of the range reduces the MSE by 30% compared to the bearing-only case.

Additionally, the aforementioned scenarios were simulated for multiple levels of angular measurements noise. The standard deviations σ_ϕ and σ_φ were varied from 10% to 150% of their original value of 4°. The remaining noise standard deviations remained the same as in the previous simulations.

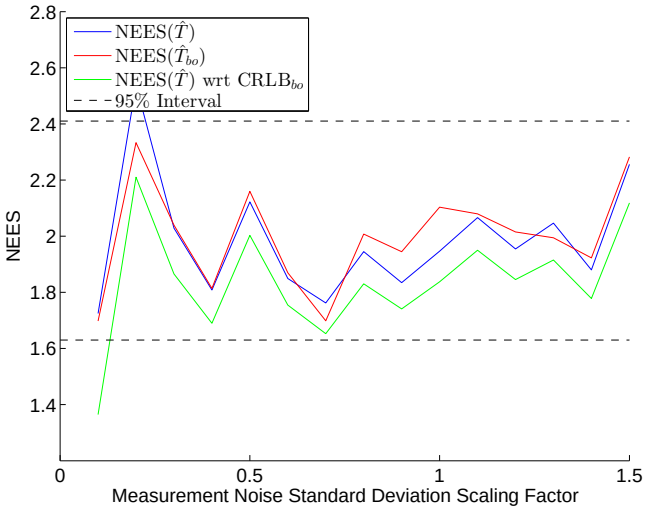

Figure 7: Scenario 1, NEES for different levels of angular measurement noise.

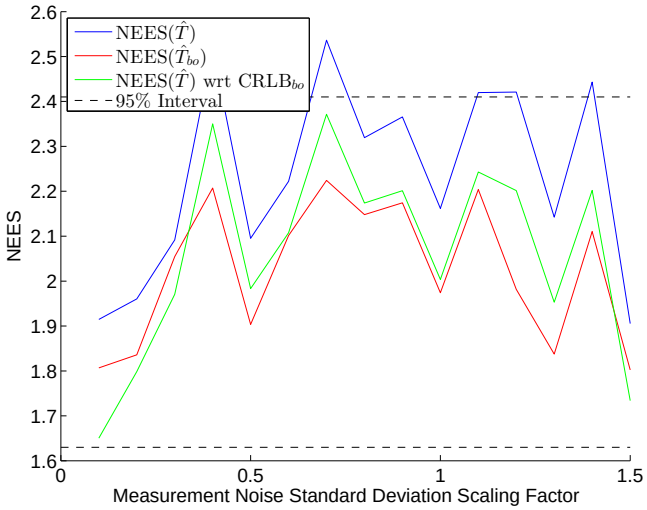

Figure 8: Scenario 2, NEES for different levels of angular measurement noise.

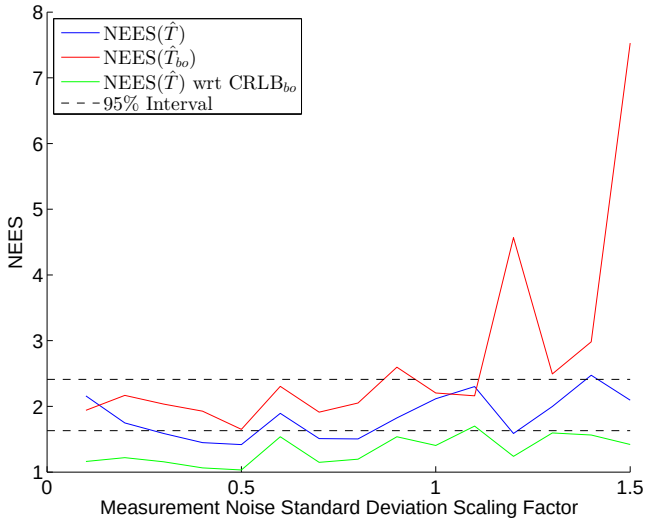

Figure 9: Scenario 3, NEES for different levels of angular measurement noise.

Figure 7 shows the NEES of Scenario 1 (from Table 1) along with the 95% confidence regions. Figures 8 and 9 show identical figures for Scenarios 2 and 3, respectively.

Figures 7–9 mirror the results of Table 1, demonstrating statistical efficiency of the fused target position estimate, with the exception of very inaccurate angular measurements and poor sensor-target geometry.

Figure 10 shows the target position RMSE (coordinate-combined) for Scenario 1, along with the CRLB, for both the bearing-only and full-position cases. This figure also shows the 95% confidence region around the CRLB for the sample RMSE over 100 Monte Carlo runs. Figures 11 and 12 show identical figures for Scenarios 2 and 3, respectively.

Figures 10 and 11 show that, over a range of angular measurement noise levels, the favorable geometry of Scenarios 1 and 2 provide for very little differentiation in the performance of target localization with or without range measurements. Figure 12 shows that, for the less favorable geometry of Scenario 3, the inclusion of range measurements provides a significant increase in the accuracy of target localization.

Additionally, the two versions of the CRLB (bearing-only and full-position) can be compared to gain insights into a particular scenario. The ratio of the area of the bearing-only CRLB ellipse to the full-position CRLB ellipse

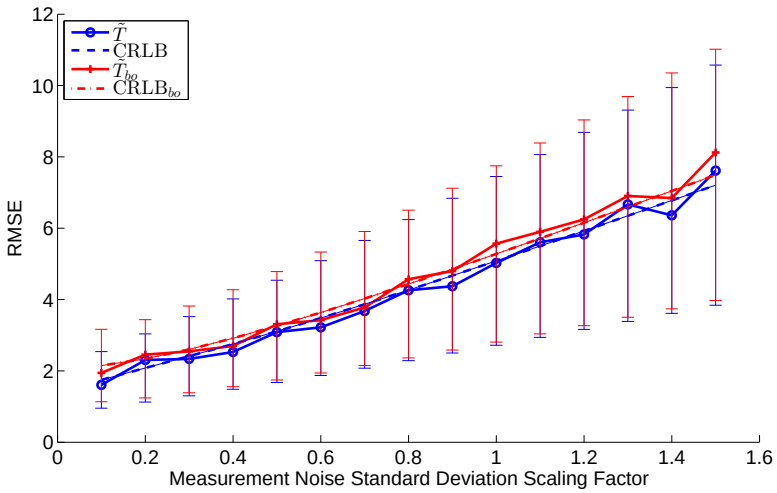

Figure 10: Scenario 1, target position RMSE for different levels of angular measurement noise and 95% probability region around the CRLB.

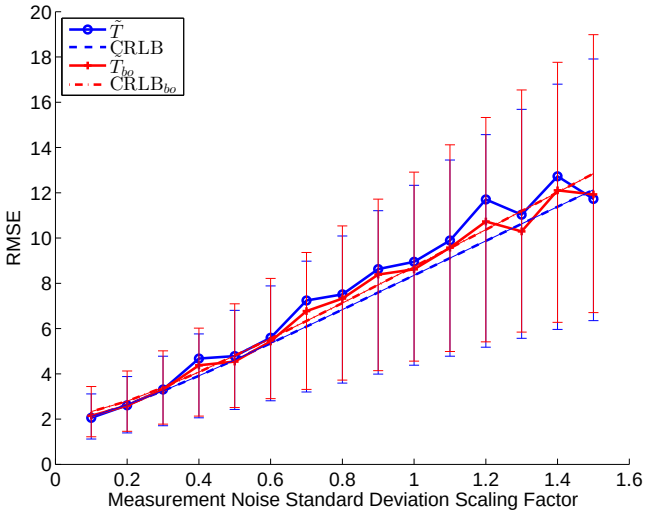

Figure 11: Scenario 2, target position RMSE for different levels of angular measurement noise and 95% probability region around the CRLB.

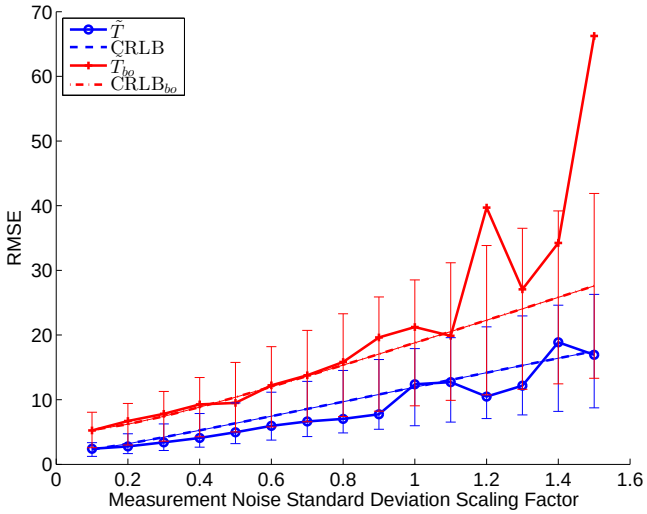

Figure 12: Scenario 3, target position RMSE for different levels of angular measurement noise and 95% probability region around the CRLB.

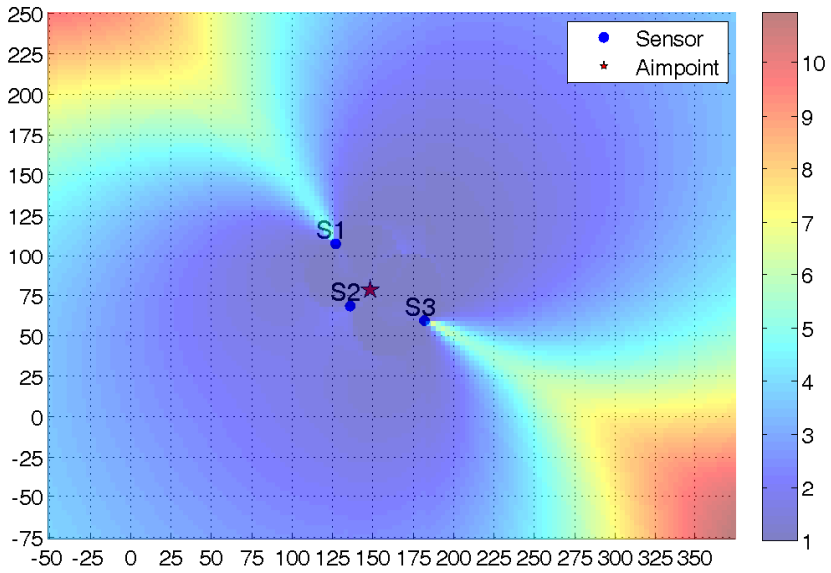

Figure 13: Comparison of CRLB and CRLB_{bo} ($|J_b^{-1}J|^{1/2}$) over a 2-d grid of shooter position (for a fixed aimpoint at $\star$).

can be calculated as $|J_b^{-1}J|^{1/2}$. This is plotted over a two-dimensional grid corresponding to various shooter locations in Figure 13, for sensor locations identical to Scenario 3. Figure 13 clearly shows the shooter locations where the range measurements are most beneficial and the bearing-only localization will perform particularly poorly.

5. CONCLUSIONS

The CRLB and statistical efficiency were examined for multiple scenarios of a localization system with position dependent noise terms; specifically, a recently developed system utilizing acoustic gunfire detection sensors [6]. The CRLB was derived for both the case of sensor nodes which send both bearing and range measurements ("full-position" CRLB) and those that do not ("bearing-only" CRLB). In cases where the sensor-target geometry is favorable for angle-only localization, the bearing-only CRLB closely matches the actual estimation errors, suggesting that there is little, if any, information contained in the range measurements in those cases. If the geometry is poor, however, as in Scenario 3, the full-position CRLB is the only one that will closely match the actual estimation errors. The results show both that the estimator used in this particular acoustic localization system is efficient, and that the full-position CRLB could act as an accurate means of performance prediction for such a system.

APPENDIX A. GENERAL FIM FOR MULTIVARIATE GAUSSIAN CASE

The FIM for the case of a multivariate Gaussian likelihood is as follows [9].

Assuming the likelihood of the parameter vector $\mathbf{x}$ given observations $\hat{\mathbf{y}}$ is distributed as $\mathcal{N}(\mu(\mathbf{x}), \Sigma(\mathbf{x}))$, the NLLF (ignoring the irrelevant constant terms) is

$$\lambda(\mathbf{x}) = \frac{1}{2}\ln|\Sigma(\mathbf{x})| + \frac{1}{2}\big(\hat{\mathbf{y}} - \mu(\mathbf{x})\big)'\Sigma(\mathbf{x})^{-1}\big(\hat{\mathbf{y}} - \mu(\mathbf{x})\big) \tag{61}$$

The gradient terms of the FIM are

$$\frac{\partial\lambda(\mathbf{x})}{\partial x_i} = \frac{1}{2}\mathrm{tr}\left(\Sigma^{-1}(\mathbf{x})\frac{\partial\Sigma(\mathbf{x})}{\partial x_i}\right) - \frac{1}{2}\big(\hat{\mathbf{y}}-\mu(\mathbf{x})\big)'\Sigma(\mathbf{x})^{-1}\frac{\partial\Sigma(\mathbf{x})}{\partial x_i}\Sigma(\mathbf{x})^{-1}\big(\hat{\mathbf{y}}-\mu(\mathbf{x})\big)' - \left[\frac{\partial\mu(\mathbf{x})}{\partial x_i}\right]'\Sigma^{-1}(\mathbf{x})\big(\hat{\mathbf{y}}-\mu(\mathbf{x})\big) \tag{62}$$

where

$$\mathbf{x} = \begin{bmatrix} x_1 & x_2 & \dots & x_n \end{bmatrix}' \tag{63}$$

The (i,j)th entry in the FIM is then

$$J_{i,j} = \frac{1}{2}\mathrm{tr}\left(\Sigma^{-1}(\mathbf{x})\frac{\partial\Sigma(\mathbf{x})}{\partial x_i}\Sigma^{-1}(\mathbf{x})\frac{\partial\Sigma(\mathbf{x})}{\partial x_j}\right) + \left[\frac{\partial\mu(\mathbf{x})}{\partial x_i}\right]'\Sigma^{-1}(\mathbf{x})\left[\frac{\partial\mu(\mathbf{x})}{\partial x_j}\right] \tag{64}$$

APPENDIX B. GRADIENT TERMS FOR BEARING-ONLY FIM

The terms of the gradient of the log-likelihood function (22), when ignoring the range measurements, are

$$\frac{\partial\lambda}{\partial T_x} = \frac{1}{\sigma_\phi^2}\sum_{i=1}^{n}\left(\hat{\phi}_i-\phi_i\right)\left(\frac{T_y-S_{i_y}}{r_i^2}\right) \tag{65}$$

$$\frac{\partial\lambda}{\partial T_y} = -\frac{1}{\sigma_\phi^2}\sum_{i=1}^{n}\left(\hat{\phi}_i-\phi_i\right)\left(\frac{T_x-S_{i_x}}{r_i^2}\right) \tag{66}$$

$$\frac{\partial\lambda}{\partial\omega} = -\frac{1}{\sigma_\varphi^2}\sum_{i=1}^{n}\left(\hat{\omega}_i-\omega\right) \tag{67}$$

$$\frac{\partial\lambda}{\partial S_{i_x}} = -\frac{1}{\sigma_\phi^2}\left(\hat{\phi}_i-\phi\right)\left(\frac{T_y-S_{i_y}}{r_i^2}\right) - \frac{1}{\sigma_{i_x}^2}\left(\hat{S}_{i_x}-S_{i_x}\right) \tag{68}$$

$$\frac{\partial\lambda}{\partial S_{i_y}} = \frac{1}{\sigma_\phi^2}\left(\hat{\phi}_i-\phi\right)\left(\frac{T_x-S_{i_x}}{r_i^2}\right) - \frac{1}{\sigma_{i_x}^2}\left(\hat{S}_{i_y}-S_{i_y}\right) \tag{69}$$

APPENDIX C. GRADIENT TERMS FOR FULL-POSITION FIM

The terms of the gradient of the log-likelihood function (22), including the range measurements, are

$$\frac{\partial\lambda}{\partial T_x} = \sum_{i=1}^{n}\left\{\left(\hat{r}_i-r_i\right)^2\alpha_i - \left(\hat{r}_i-r_i\right)\left(\frac{T_x-S_{i_x}}{r_i\sigma_{r_i}^2}\right) - \sigma_{r_i}^2\alpha_i\right\} + \frac{1}{\sigma_\phi^2}\sum_{i=1}^{n}\left(\hat{\phi}_i-\phi_i\right)\left(\frac{T_y-S_{i_y}}{r_i^2}\right) \tag{70}$$

$$\frac{\partial\lambda}{\partial T_y} = \sum_{i=1}^{n}\left\{\left(\hat{r}_i-r_i\right)^2\beta_i - \left(\hat{r}_i-r_i\right)\left(\frac{T_y-S_{i_y}}{r_i\sigma_{r_i}^2}\right) - \sigma_{r_i}^2\beta_i\right\} - \frac{1}{\sigma_\phi^2}\sum_{i=1}^{n}\left(\hat{\phi}_i-\phi_i\right)\left(\frac{T_x-S_{i_x}}{r_i^2}\right) \tag{71}$$

$$\frac{\partial\lambda}{\partial\omega} = \sum_{i=1}^{n}\left(\hat{r}_i-r_i\right)^2\gamma_i - \sigma_{r_i}^2\gamma_i - \frac{1}{\sigma_\varphi^2}\left(\hat{\omega}_i-\omega\right) \tag{72}$$

$$\frac{\partial\lambda}{\partial S_{i_x}} = -\left(\hat{r}_i-r_i\right)^2\alpha_i + \left(\hat{r}_i-r_i\right)\left(\frac{T_x-S_{i_x}}{r_i\sigma_{r_i}^2}\right) + \sigma_{r_i}^2\alpha_i - \frac{1}{\sigma_\phi^2}\left(\hat{\phi}_i-\phi\right)\left(\frac{T_y-S_{i_y}}{r_i^2}\right) - \frac{1}{\sigma_{i_x}^2}\left(\hat{S}_{i_x}-S_{i_x}\right) \tag{73}$$

$$\frac{\partial\lambda}{\partial S_{i_y}} = -\left(\hat{r}_i-r_i\right)^2\beta_i + \left(\hat{r}_i-r_i\right)\left(\frac{T_y-S_{i_y}}{r_i\sigma_{r_i}^2}\right) + \sigma_{r_i}^2\beta_i + \frac{1}{\sigma_\phi^2}\left(\hat{\phi}_i-\phi\right)\left(\frac{T_x-S_{i_x}}{r_i^2}\right) - \frac{1}{\sigma_{i_x}^2}\left(\hat{S}_{i_y}-S_{i_y}\right) \tag{74}$$

where

$$\alpha_i = \big(T_y - S_{i_y}\big)\left(\frac{(\sigma_\phi^2+\sigma_\varphi^2)\sin(\phi_i-\varphi_i)\cos(\phi_i-\varphi_i)}{\big(1-\cos(\phi_i-\varphi_i)\big)^2\sigma_{r_i}^4} - \frac{\sin(\phi_i-\varphi_i)}{r_i^2\big(1-\cos(\phi_i-\varphi_i)\big)\sigma_{r_i}^2}\right) - \big(T_x - S_{i_x}\big)\frac{(\sigma_\phi^2+\sigma_\varphi^2)\sin^2(\phi_i-\varphi_i)}{\big(1-\cos(\phi_i-\varphi_i)\big)^2\sigma_{r_i}^4} \tag{75}$$

$$\beta_i = \big(T_x - S_{i_x}\big)\left(-\frac{(\sigma_\phi^2+\sigma_\varphi^2)\sin(\phi_i-\varphi_i)\cos(\phi_i-\varphi_i)}{\big(1-\cos(\phi_i-\varphi_i)\big)^2\sigma_{r_i}^4} + \frac{\sin(\phi_i-\varphi_i)}{r_i^2\big(1-\cos(\phi_i-\varphi_i)\big)\sigma_{r_i}^2}\right) - \big(T_y - S_{i_y}\big)\frac{(\sigma_\phi^2+\sigma_\varphi^2)\sin^2(\phi_i-\varphi_i)}{\big(1-\cos(\phi_i-\varphi_i)\big)^2\sigma_{r_i}^4} \tag{76}$$

$$\gamma_i = \frac{r_i^2(\sigma_\phi^2+\sigma_\varphi^2)\sin(\phi_i-\varphi_i)\cos(\phi_i-\varphi_i)}{(1-\cos(\phi_i-\varphi_i))^2\sigma_{r_i}^4} - \frac{\sin(\phi_i-\varphi_i)}{(1-\cos(\phi_i-\varphi_i))\sigma_{r_i}^2} \tag{77}$$

REFERENCES

[1] Y. Bar-Shalom, X.-R. Li, and T. Kirubarajan, *Estimation with Applications to Tracking and Navigation: Theory, Algorithms and Software*. J. Wiley and Sons, 2001.

[2] J. L. Crassidis, R. Alonso, and J. L. Junkins, "Optimal Attitude and Position Determination from Line-of-Sight Measurements," *Journal of the Astronautical Sciences*, vol. 48(2), pp. 391–408, 2000.

[3] D. F. Crouse, R. W. Osborne, III, K. Pattipati, P. Willett, and Y. Bar-Shalom, "2D Location Estimation of Angle-Only Sensor Arrays Using Targets of Opportunity," in *13th International Conference on Information Fusion*, Edinburgh, UK, Jul. 2010, pp. 1–8.

[4] W. H. Foy, "Position-Location Solutions by Taylor-Series Estimation," *IEEE Trans. on Aerospace and Electronic Systems*, vol. 12(2), pp. 187–194, Mar. 1976.

[5] M. Gavish and A. J. Weiss, "Performance Analysis of Bearing-Only Target Location Algorithms," *IEEE Trans. on Aerospace and Electronic Systems*, vol. 28(3), pp. 817–828, Jul. 1992.

[6] J. George and L. M. Kaplan, "Shooter Localization using Soldier-Worn Gunfire Detection Systems," in *14th International Conference on Information Fusion*, Chicago, IL, Jul. 2011, pp. 398–405.

[7] L. M. Kaplan, T. Damarla, and T. Pham, "QoI for Passive Acoustic Gunfire Localization," in *Mobile Ad Hoc and Sensor Systems, 2008. MASS 2008. 5th IEEE International Conference on*, Oct. 2008, pp. 754–759.

[8] R. W. Osborne, III and Y. Bar-Shalom, "Statistical Efficiency of Composite Position Measurements from Passive Sensors," in *Proc. SPIE Conf. Signal Processing, Sensor Fusion and Target Recognition*, vol. 8050-07, Orlando, FL, Apr. 2011.

[9] B. Porat and B. Friedlander, "Computation of the Exact Information Matrix of Gaussian Time Series with Stationary Random Components," *IEEE Trans. on Acoustics, Speech, and Signal Processing*, vol. 34, no. 1, pp. 118–130, Feb. 1986.

[10] D. J. Torrieri, "Statistical Theory of Passive Location Systems," *IEEE Trans. on Aerospace and Electronic Systems*, vol. 20(2), pp. 183–198, Mar. 1984.

[11] M. Wax, "Position Location from Sensors with Position Uncertainty," *IEEE Trans. on Aerospace and Electronic Systems*, vol. 19(5), pp. 658–662, Sep. 1983.

[12] Y. Zhao, D. Yi, Y. Li, and Q. Zhang, "CRLB of Initial State Estimation for Boost Phase Object Based on 8-State Gravity Turn Model Using Space-Based Observations," in *2010 2nd International Conference on Signal Processing Systems (ICSPS)*, vol. 1, Dalian, China, Jul. 2010, pp. 781–789.